

# An iterative denoising system based on Wiener filtering with application to biomedical images



Salim Lahmiri

Department of electrical engineering, École de Technologie Supérieure, Montreal, Canada

## ARTICLE INFO

### Keywords:

Biomedical images  
Denoising  
Wiener filter  
Iterative system  
Peak-signal-to-noise-ratio

## ABSTRACT

Biomedical image denoising systems are important for accurate clinical diagnosis. The purpose of this study is to present a simple and effective iterative multistep image denoising system based on Wiener filtering (WF) where the denoised image from one stage is the input to the next stage. The denoising process stops when a particular condition measured by image energy is adaptively achieved. The proposed iterative system is tested on real clinical images and performance is measured by the well-known peak-signal-to-noise-ratio (PSNR) statistic. Experimental results showed that the proposed iterative system outperforms conventional image denoising algorithms; including wavelet packet (WP), fourth order partial differential equation (FOPDE), nonlocal Euclidean means (NLEM), first order local statistics (FOLS), and single Wiener filter used as baseline model. The experimental results demonstrate that the proposed approach can remove noise automatically and effectively while edges and texture characteristics are preserved.

## 1. Introduction

Image enhancement and denoising are usually used to better visualize and interpret the content [1–6]. In this regard, several effective denoising systems for enhancement of biomedical images corrupted with noise during acquisition process have been proposed in the literature. The main goal of biomedical image denoising is to suppress noise from acquired image while preserving as much as possible its meaningful edges or texture details. Indeed, the accuracy of clinical diagnosis depends mainly on visual quality of acquired images. For instance, wavelet-based approach was adopted in [7], partial differential equation was employed in [8,9], adjusted empirical mode decomposition in [10], nonlocal means in [11], and Wiener filter was used in [12]. As a suitable filter to reduce the effects of non-stationary noise, Wiener filter was successful in denoising one and two dimensional biomedical signals [13,14], and also in image processing in general [15].

Recently, several iterative approaches were proposed in the literature to denoise images. For instance, an iterative method based on fuzzy sub-pixel fractional partial difference was proposed in [16]. The proposed iterative method was successful in enhancing contrast of noisy image. However, it is a computationally complex method [16]. An iterative generalized cross-validation and fast translation invariant approach for image denoising was proposed in [17]. The approach is based on wavelet thresholding algorithm and found to be fast and effective as it reduces the computation cost of the standard generalized

cross-validation method and efficiently suppresses the Pseudo-Gibbs phenomena. However, it yields to slight blurring due to simplicity of the soft-threshold function which is necessary to accelerate computation. The authors in [18] proposed a noise adjusted iterative low-rank matrix approximation method. For instance, a patchwise randomized singular value decomposition is first applied to denoise the image. Then, an iterative regularization technique based on low-rank matrix approximation is employed to further separate the signal and noise. The proposed algorithm requires an appropriate stopping parameter to be pre-determined along with number of iterations. More recently, the authors in [19] proposed an automatic filtering convergence method using PSNR checking and filtered pixel detection for iterative impulse noise filters by defining an adaptive stop criterion to filter a corrupted image within finite steps. However, the improved iterative impulse noise filters fail to discriminate both impulse noise and high-frequency signal contained in high-frequency image.

In this paper, a simple and effective multistep system for image denoising based on Wiener filtering is presented. The Wiener filter is chosen as the basis of our proposed multistep denoising system for three reasons. First, it is effective in reducing the effects of non-stationary noise [14]. Second, it incorporates both the degradation function and statistical characteristics of noise into the restoration process [15]. Third, it can remove the additive noise and invert the blurring simultaneously [15].

The proposed multistep system for image denoising based on Wiener filtering is described as follows. In the first step, the Wiener

E-mail address: [salim.lahmiri.1@ens.etsmtl.ca](mailto:salim.lahmiri.1@ens.etsmtl.ca).

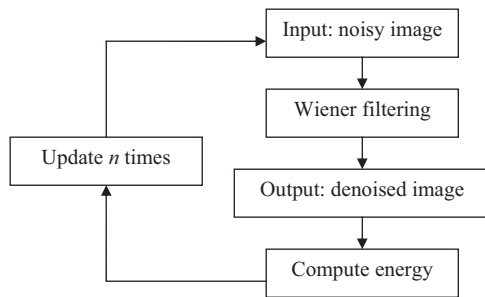


**Fig. 1.** Block diagram of the proposed multistage denoising system. The procedure is repeated until there is a decrease in energy of the denoised image.

filter is applied to the noisy image. In the second step, the obtained denoised image in previous step is processed by Wiener filter for improving image quality by removing the remaining noise. The resulting denoised image in second step is further processed by Wiener filter in third step. In other words, the proposed denoising system is composed of several stages/steps where each obtained denoised image is further processed with Wiener filter. The process continues until obtaining a better quality of the image. For instance, the multistep processing stops when a given condition is automatically satisfied.

In order to evaluate the proposed multistep denoising system, a set of three biomedical images is considered. In particular, the real clinical test images are degraded by various levels of Gaussian noise. In addition, the effectiveness of the proposed multistage denoising system is compared with that of conventional existing methods; including wavelet packet (WP) [20], fourth order partial differential equation (PDE) [21], nonlocal Euclidean mean (NLEM) [22], and first order local statistics (FOLS) [23]. Finally, the performances of all algorithms will be evaluated in terms of the well-known peak-signal-to-noise ratio (PSNR).

The remainder of this paper is organized as follows: Section 2 presents our proposed multistep denoising system along with comparison techniques. Section 3 presents the experimental results. Finally, Section 4 concludes our study.

## 2. Methods

In this section, our multistep denoising system and comparison methods are presented. In addition, the peak-signal-to-noise ratio used as main performance measure is presented.

### 2.1. Proposed multistep system based on Wiener filtering

In order to provide a good quality of denoised biomedical image, we build a multistage denoising system based on several iterations of Wiener filter. Indeed, the goal is to iteratively apply Wiener filter to obtained denoised images until expected denoising performance stops improving. For instance, the Wiener filter is applied to the initial noisy

image in the first iteration. The obtained denoised image in previous iteration is filtered by Wiener filter in the second iteration. The resulting denoised image in second iteration step is further processed by Wiener filter in third iteration; and so on. The number of iterations is not fixed, but is adaptive as the overall denoising process automatically stops when energy of the denoised image in iteration  $n$  is smaller than that in iteration  $n-1$ . In this regard, there is no further improvement in the denoising outcome.

The algorithm of the proposed Wiener-based system for image denoising is described as follows:

- Apply Wiener filter to noisy image.
- Compute energy ( $E_1$ ) of the denoised image.
- Apply Wiener filter to denoised image obtained in (b).
- Compute  $E_2$  of the denoised image in (c).
- If  $E_2 > E_1$  then apply Wiener filter to denoised image obtained in (c) and continue to next stage  $n$ ; else stop. This is the update stage.
- Repeat (b) to (e)  $n$  times until  $E_n < E_{n-1}$

For illustration purpose, the proposed multistep (iterative) denoising system based on Wiener filtering is summarized in Fig. 1:

The Wiener filter [24] is an adaptive technique based on local mean ( $\mu$ ) and variance ( $\sigma^2$ ) around each pixel of a noisy image  $a(n_1, n_2)$ . In particular, Wiener filter creates a pixel wise filtering using estimated mean and variance to obtain an estimated or denoised image  $b(n_1, n_2)$  given by:

$$E(u) = \int_{\Omega} f(|\nabla^2 u|) dx dy. \quad (1)$$

where  $v^2$  is the noise variance that could be estimated as average of all local estimated variances.

The methods used for comparison purpose; namely the wavelet packet (WP) [20], fourth order partial differential equation (PDE) [21], nonlocal Euclidean means (NLEM) [22], and first order local statistics (FOLS) [23]; are described next.

### 2.2. Comparison methods and performance measure

Following the classical approach for image denoising based on wavelet transform, the noisy image is decomposed by using discrete wavelet transform (DWT) [25] to decompose it into low-low, low-high, high-low, and high-high sub-band coefficients. The denoised signal is obtained by thresholding the obtained wavelet coefficients. Then, an inverse DWT is performed to recover the denoised signal. In this paper, wavelet packet transform (WPT) [20,26] that performs a complete analysis of the image at all subbands including both approximation and detail coefficients; is employed for denoising purpose. For the WPT thresholding technique, we employ the Daubechies-4 as mother wavelet at third level of decomposition. The optimal threshold value is determined by minimizing Stein's unbiased risk estimator (SURE) [25]. Indeed, denoising by wavelet transform is usually performed by thresholding where coefficients smaller than a specific threshold are

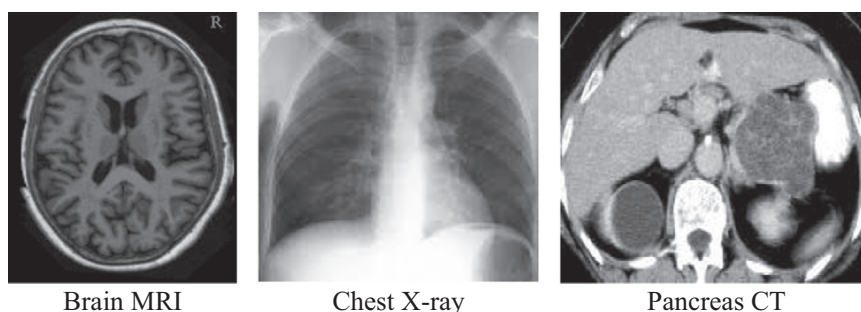


**Fig. 2.** Original images used for experiments.

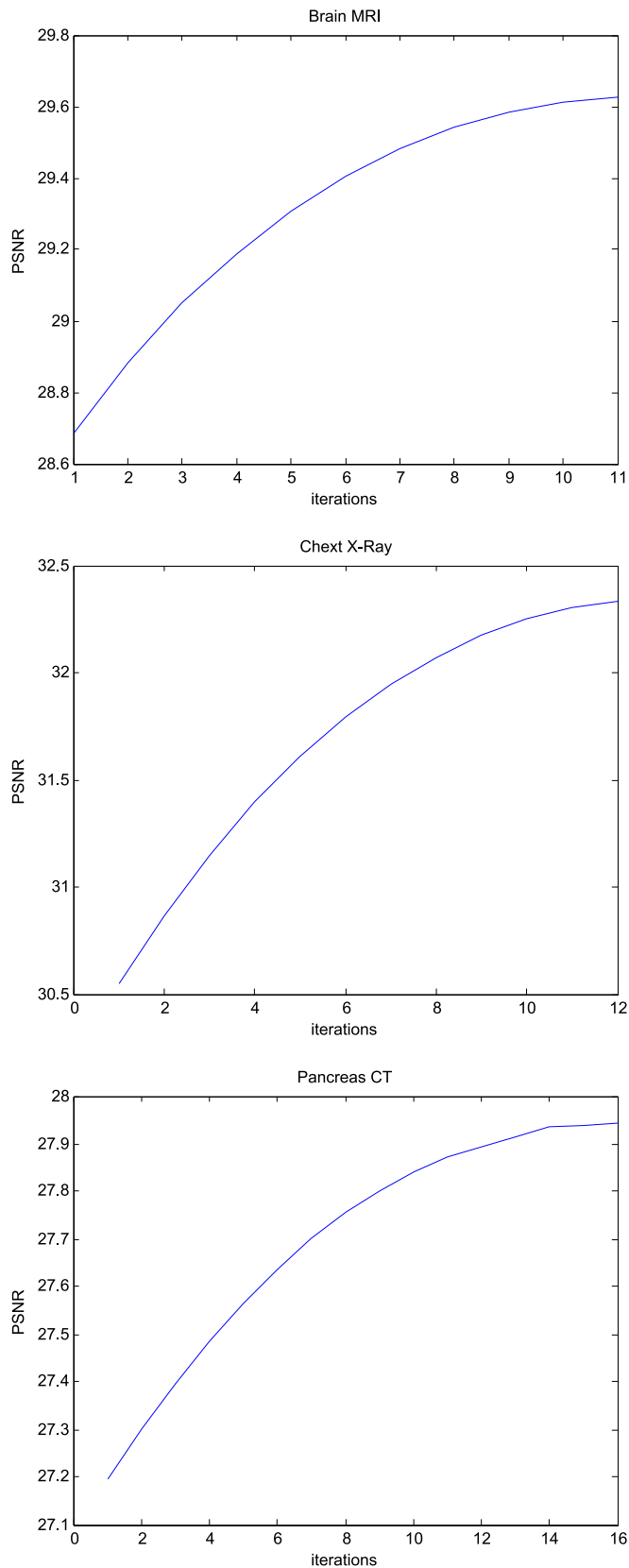


Fig. 3. PSNR given number of iterations under S3.

canceled [25]. Two types of thresholding are in general applied: Hard and soft thresholding. The former replaces wavelet coefficients less than the threshold with zero. The latter, replaces wavelet coefficients less than the threshold with zero and the remaining coefficients are

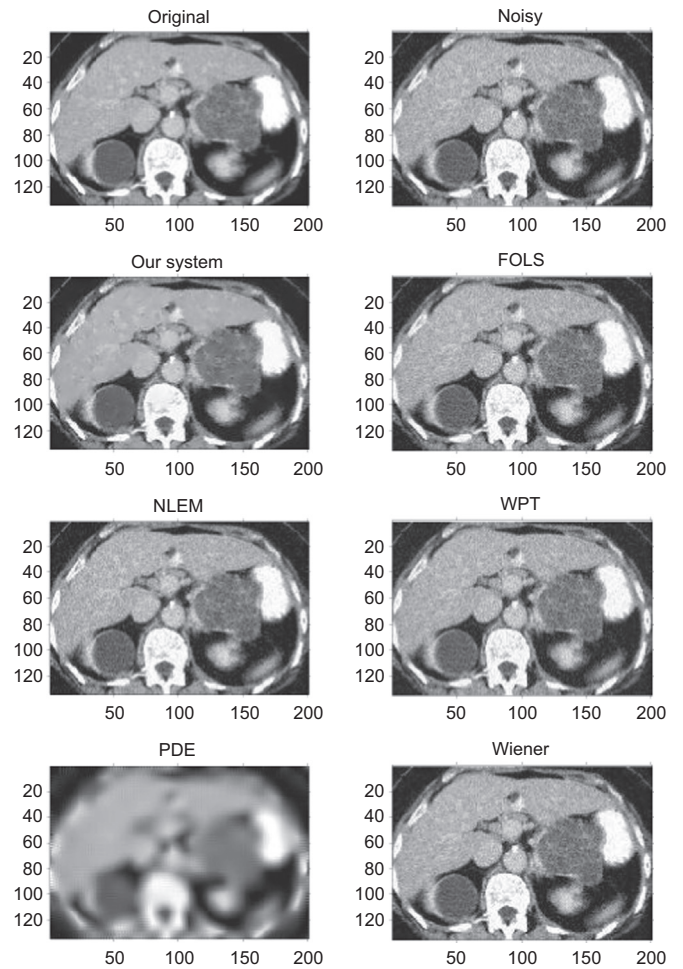


Fig. 4. Resulting denoised images under S1 for pancreas CT.

modified by subtracting the threshold value. Both types of thresholding are adopted in this study.

The PDE denoising approach [21] is based on the principle of cost function minimization. For  $(x,y) \in \Omega$ , let  $u(x,y)$  and  $u_0(x,y)$  be respectively a digital image and its observation with random noise  $\varepsilon(x,y)$ . The purpose is to find a new image by minimizing the cost functional  $E(u)$  given by [21]:

$$E(u) = \int_{\Omega} f(|\nabla^2 u|) dx dy \quad (2)$$

where  $\nabla^2$  is the Laplacian operator and  $f(\cdot) \geq 0$  and also  $f'(\cdot) > 0$ . With the observed image as the initial condition, the solution is given by the following PDE as the time script tends to infinity:

$$\frac{\partial u}{\partial t} = -\nabla^2 \left[ f'(\nabla^2 u) \frac{\nabla^2 u}{|\nabla^2 u|} \right] \quad (3)$$

In the nonlocal Euclidean means (NLEM) framework [22], the Euclidean mean is the minimizer of.

$\sum_j w_j \| \mathbf{P} - \mathbf{P}_j \|^2$  over all image patches  $\mathbf{P}$  of size  $k \times k$  centered at pixel  $j$ . The nonlocal Euclidean medians (NLEM) method [22] seeks to minimize.

$\sum_j w_j \| \mathbf{P} - \mathbf{P}_j \|$  over all  $\mathbf{P}$ ; as the median is more robust to outliers than the mean, by using the iteratively reweighted least squares (IRLS) algorithm [22].

First order local statistics (FOLS) [23] filter estimates pixel characteristics by calculating sub-region statistics estimated over a neighborhood  $W$ . The filter is expressed as follows [23]:

$$\hat{f}_{i,j} = \bar{g}_{i,j} + k_{i,j}(g_{i,j} - \bar{g}_{i,j}) \quad (4)$$

**Table 1**  
PSNR values of different denoising methods.

	Brain MRI			Chest x-ray			Pancreas CT		
	S1	S2	S3	S1	S2	S3	S1	S2	S3
PDE	16.61	16.55	16.30	28.68	28.60	28.37	19.27	19.23	19.19
FOLS	28.32	25.42	24.94	32.39	29.03	26.98	30.79	27.80	26.18
NLEM	28.47	25.53	25.04	30.13	27.17	25.46	30.56	27.50	25.83
WPT	28.69	25.65	25.04	30.49	27.44	25.71	30.76	27.70	26.03
Single Wiener	31.53	28.44	28.69	34.60	32.11	30.55	31.24	29.56	27.20
Proposed	<b>32.31</b>	<b>29.66</b>	<b>29.63</b>	<b>35.66</b>	<b>33.56</b>	<b>32.33</b>	<b>31.82</b>	<b>29.60</b>	<b>27.94</b>

where  $f_{i,j}$  is the estimated pixel at location  $(i,j)$  on the image with an original value of  $g_{i,j}$ ,  $\bar{g}_{i,j}$  is gray value local mean of an  $m \times n$  neighborhood around and including  $g_{i,j}$ ;  $k_{i,j}$  is the weighing factor with  $k \in [0,1]$ . The factor  $k_{i,j}$  is expressed as [23]:

$$k_{i,j} = \frac{1 - \bar{g}_{i,j}^2 \sigma_{i,j}^2}{\sigma_{i,j}^2 (1 + \sigma^2)} \quad (5)$$

$$\sigma^2 = \sum_{i,j} \frac{\sigma_{i,j}^2}{\bar{g}_{i,j}} \quad (6)$$

where  $\sigma_{i,j}^2$  and  $\sigma^2$  are respectively local noise variance in the moving window  $W$  and noise variance in the whole image. In this study, a local neighborhood window  $W$  of size  $5 \times 5$  is considered.

Finally, the denoising performance is measured by the peak-signal-to-noise ratio (PSNR) given by:

$$PSNR = 20 \log_{10} \left( \frac{MAX_f}{\sqrt{MSE}} \right) \quad (7)$$

where, MAX is the maximum signal value in the original image  $f$  of size  $m \times n$ , and MSE is the mean squared error.

### 3. Results

In this section, the performance of the proposed multistep denoising system in terms of PSNR is compared to wavelet packet (WP), fourth order partial differential equation (PDE), nonlocal Euclidean mean (NLEM), first order local statistics (FOLS), and also to single (one iteration) Wiener filter. They were applied to three biomedical images: brain MRI (256×256), pancreas computed tomography (CT) (275×183), and chest X-ray image (180×176). Fig. 2 displays the original biomedical images used in our experiments. A Gaussian noise was added to each biomedical image at varying levels. For instance, the noise had a normal distribution with zero mean and standard deviation S1=0.01, S2=0.02, and S3=0.03. Fig. 3 plots the evolution of PSNR depending on number of iterations in our proposed multistep denoising system when biomedical images shown in Fig. 2 are corrupted with noise of level S1. It is shown that the PSNR increases with number of iterations. We found similar results when original biomedical images were corrupted with noise of levels S2 and S3. These findings suggest that applying Wiener filter iteratively to obtained images improves the denoising result. Thus, the proposed multistep denoising system based on iterative Wiener filtering is capable to improve its performance automatically and adaptively. Recall, that our system automatically stops when energy of the denoised image decreases.

For visual quality comparison, the resulting images through all denoising models adopted in our study for pancreas CT affected with Gaussian noise level S1 are shown in Fig. 4. It is observed that the proposed multistep denoising system based on Wiener filtering performs better than the existing methods by providing better visual quality of the denoised image.

In addition to that, the obtained PSNR by the proposed multistep denoising system and existing comparison methods are provided in

Table 1 for brain MRI, chest X-ray, and pancreas CT respectively. Recall that hard and soft threshold achieved similar performances. From Table 1, it is observed that our proposed multistep denoising system performs better than the other methods in terms of PSNR. In summary, compared to other denoising models used for comparison purpose, our proposed multistep denoising system based on iterative Wiener filtering allows enhancing the contrast of the image with better preservation of edge and important details as clearly shown in Fig. 3. Therefore, our filtering system tends to produce good denoised image not only in terms of visual perception but also in terms of the PSNR metric. Fig. 4

Overall, the PDE based approach is able to preserve object boundaries while removing noise in homogeneous regions. But, it requires numerical methods to be solved and yields to blurred regions. FOLS and NLEM are capable to remove noise from smooth regions; however, they fail to provide good results close to edge regions. As a wavelet-based image denoising method, the WPT can preserve texture and details but it produces artifacts. Besides, the proposed iterative denoising approach based on Wiener filter has several advantages. In particular, the proposed system is simple to implement and fast as no prior processing step is required. In addition, the proposed iterative denoising system is capable to remove noise from an image adaptively in finite iterations while important image characteristics are preserved such as edges and texture. Indeed, since Wiener filter acts locally to remove additive noise and invert the blurring simultaneously [15], image local characteristics are prevailed. Thus, it is suitable for restoring original textural features. Furthermore, our proposed iterative denoising system was found to be effective in comparison with existing denoising techniques used for comparison purpose. Finally, it is interesting to notice that although Wiener filter is suitable for smooth images, it also worked well for non-smooth images under study when used in an iterative framework. Such advantages are attractive in real world applications; particularly, in clinical applications for better diagnosis.

### 4. Conclusion

Biomedical image denoising systems are important in clinical diagnosis as images acquired through electronic sensors may be contaminated by noise. In this regard, biomedical image denoising systems are employed for biomedical image enhancement at a pre-processing step.

In this study, we constructed a simple an effective automated biomedical denoising system based on multistage usage of Wiener filter. We compared the performance of our proposed multistage denoising system to wavelet packet, fourth order partial differential equation, nonlocal Euclidean means, first order local statistics, and single Wiener filtering. Experimental results showed that our multistep system based on Wiener filtering achieved best performances in terms of both subjective and objective evaluations than comparison models.

## References

- [1] M.K. Sharma, J. Joseph, P. Senthilkumaran, Directional edge enhancement using superposed vortex filter, *Opt. Laser Technol.* 57 (2014) 230–235.
- [2] X. Bai, F. Zhou, B. Xue, Image enhancement using multiscale image features extracted by top-hat transform, *Opt. Laser Technol.* 44 (2012) 328–336.
- [3] Y. Li, Y. Zhang, A. Geng, L. Cao, J. Chen, Infrared image enhancement based on atmospheric scattering model and histogram equalization, *Opt. Laser Technol.* 83 (2016) 99–107.
- [4] H. Om, M. Biswas, MMSE based map estimation for image denoising, *Opt. Laser Technol.* 57 (2014) 252–264.
- [5] P. Shanmugavadivu, K. Balasubramanian, Particle swarm optimized multi-objective histogram equalization for image enhancement, *Opt. Laser Technol.* 57 (2014) 243–251.
- [6] M. Liao, Y.-q. Zhao, X.-h. Wang, P.-s. Dai, Retinal vessel enhancement based on multi-scale top-hat transformation and histogram fitting stretching, *Opt. Laser Technol.* 58 (2014) 56–62.
- [7] T. Bernas, R. Starosolski, R. Wójcicki, Application of detector precision characteristics for the denoising of biological micrographs in the wavelet domain, *Biomed. Signal Process. Control* 19 (2015) 1–15.
- [8] J.M. Bioucas-Dias, M.A.T. Figueiredo, Multiplicative noise removal using variable splitting and constrained optimization, *IEEE Trans. Image Process.* 19 (2010) 1720–1730.
- [9] S. Lahmiri, Image denoising in bidimensional empirical mode decomposition domain: the role of Student's probability distribution function, *Healthc. Technol. Lett.* 3 (2016) 67–71.
- [10] S.Lahmiri, M.Boukadoum, Combined partial differential equation filtering and particle swarm optimization for noisy biomedical image segmentation, in: *Proceedings of the IEEE Latin American Symposium on Circuits and Systems*, pp. 363–366, 2016.
- [11] S. Duli, A. Kuurstra, I.C.S. Patarroyo, O.V. Michailovich, A new similarity measure for non-local means filtering of MRI images, *J. Vis. Commun. Image Represent.* 24 (2013) 1040–1054.
- [12] X.-W. Fu, M.-Y. Ding, C. Cai, Despeckling of medical ultrasound images based on quantum-inspired adaptive threshold, *Electron. Lett.* 46 (2010) 889–891.
- [13] L. Smital, M. Vitek, J. Kozumplik, I. Provazník, Adaptive wavelet Wiener filtering of ECG signals, *Trans. Biomed. Eng.* 60 (2013) 437–445.
- [14] Q. Xu, D. Ye, Evaluation of a posteriori Wiener filtering applied to frequency-following response extraction in the auditory brainstem, *Biomedical, Signal Process. Control* 14 (2014) 206–216.
- [15] J.-C. Yoo, C.W. Ahn, Image restoration by blind-Wiener filter, *IET Image Process.* 8 (2014) 815–823.
- [16] Y. Zhang, H.D. Cheng, J. Tian, J. Huang, X. Tang, Fractional subpixel diffusion and fuzzy logic approach for ultrasound speckle reduction, *Pattern Recognit.* 43 (2010) 2962–2970.
- [17] Libao Zhang, Jie Chen, Tong Zhu, Image denoising based on iterative generalized cross-validation and fast translation invariant, *J. Vis. Commun. Image Represent.* 28 (2015) 1–14.
- [18] W. He, H. Zhang, L. Zhang, H. Shen, Hyperspectral image denoising via noise-adjusted iterative low-rank matrix approximation, *IEEE J. Sel. Top. Appl. Earth Obs. Remote Sens.* 8 (2015) 3050–3061.
- [19] C.-Y. Chen, C.-H. Chen, C.-H. Chen, K.-P. Lin, An automatic filtering convergence method for iterative impulse noise filters based on PSNR checking and filtered pixels detection, *Expert Syst. Appl.* 63 (2016) 198–207.
- [20] P.L. Shui, Z.F. Zhou, J.X. Li, Image denoising algorithm via best wavelet packet base using Wiener cost function, *IET Image Process.* 1 (2007) 311–318.
- [21] Y.-L. You, M. Kaveh, Fourth order partial differential equations for noise removal, *IEEE Trans. Image Process.* 9 (2000) 1723–1730.
- [22] D. Sheet, S. Pal, A. Chakraborty, J. Chatterjee, A.K. Ray, Image quality assessment for performance evaluation of despeckle filters in optical coherence tomography of human skin, *Proc. IEEE EMBS* (2010) 499–504.
- [23] J.S. Lee, Digital image smoothing and sigma filter, *Comput. Vis. Graph. Image Process.* 24 (1983) 255–269.
- [24] M. Kazubek, Wavelet domain image denoising by thresholding and Wiener filtering, *IEEE Signal Process. Lett.* 10 (2003) 324–326.
- [25] D.L. Donoho, De-noising by soft-thresholding, *IEEE Trans. Inf. Theory* 41 (1995) 613–627.
- [26] M.V. Wickerhauser, R.R. Coifman, Entropy-based algorithms for best basis selection, *IEEE Trans. Inf. Theory* 38 (1992) 713–718.